

# Differential Association of Phosphodiesterase 4D Isoforms with $\beta_2$ -Adrenoceptor in Cardiac Myocytes\*<sup>§</sup>

Received for publication, May 13, 2009, and in revised form, September 22, 2009 Published, JBC Papers in Press, October 1, 2009, DOI 10.1074/jbc.M109.020388

Vania De Arcangelis<sup>‡</sup>, Ruijie Liu<sup>‡</sup>, Dagoberto Soto<sup>‡</sup>, and Yang Xiang<sup>†§1</sup>

From the <sup>‡</sup>Department of Molecular and Integrative Physiology and <sup>§</sup>Neuroscience Program, University of Illinois at Urbana-Champaign, Urbana, Illinois 61801

cAMP and protein kinase A (PKA) activation represents a key signaling mechanism upon  $\beta$ -adrenergic stimulation under stress. Both  $\beta_1$ - and  $\beta_2$ -adrenoreceptor (ARs) subtypes induce cAMP accumulation, yet play distinct roles in cardiac contraction and myocyte apoptosis. Differences in controlling cAMP/PKA activities through the assembly of complexes between the receptors and cAMP-specific phosphodiesterases contribute to the distinct biological outcomes. Here, we demonstrate that  $\beta_2$ ARs form signaling complexes with a set of PDE4D isoforms expressed in cardiac myocytes. PDE4D9 and PDE4D8 bind to the  $\beta_2$ AR at resting conditions; however, agonist stimulation induces dissociation of PDE4D9 from the receptor but recruitment of PDE4D8 to the receptor. Agonist stimulation also induces recruitment of PDE4D5 to the  $\beta_2$ AR. Moreover, the receptor-associated PDE4D isoforms play distinct roles in controlling cAMP activities and regulating the PKA phosphorylation of the receptor and myocyte contraction rate responses. Knockdown of PDE4D9 with short hairpin RNA enhances the  $\beta_2$ AR-induced cAMP signaling, whereas knockdown of PDE4D8 only slightly prolongs the receptor-induced cAMP signaling in myocytes. Inhibition of PDE4D9 and PDE4D5 enhances the base-line levels of contraction rates, whereas inhibition of PDE4D9 and PDE4D8 enhances the maximal contraction rate increases upon activation of  $\beta_2$ AR. Our data underscore the complex regulation of intracellular cAMP by  $\beta_2$ AR-associated phosphodiesterase enzymes to enforce the specificity of the receptor signaling for physiological responses.

cAMP/PKA<sup>2</sup> activation represents a key signaling mechanism upon stimulation of G protein-coupled receptors for cardiac contraction and energy metabolism under stress conditions. Activation of  $\beta$ ARs, a group of prototypical G protein-coupled receptors, is one of the major neurohormonal mechanisms controlling cAMP/PKA activities for

physiological responses in animal hearts (1).  $\beta_1$ AR and  $\beta_2$ AR are highly homologous receptors expressed in animal heart for enhancing cardiac performance.  $\beta_1$ AR plays a dominant role in stimulating heart rate and strength of myocyte contraction, whereas  $\beta_2$ AR produces only modest chronotropic effects (1). One of the emerging mechanisms that safeguard the specificity of G protein-coupled receptor/cAMP signaling is the control of cAMP transients via degradation by cyclic nucleotide PDEs (2).

PDEs include 11 families based on their amino acid sequence homology, substrate specificities, and pharmacological properties (2). Each of the 11 PDE families has one to four distinct genes. In addition, most PDE genes encode for multiple splicing variants through the usage of multiple promoters and alternative splicing. In animal hearts, PDE4 and PDE3 are two major families expressed, which account for more than 90% of PDE activities (3). These PDEs play a critical role for the subcellular specificity in cAMP signaling by preventing diffusion of cAMP from one microdomain to another (4, 5).

Our previous studies have identified that PDE4 is the major family that controls cAMP accumulation induced by both  $\beta_1$ - and  $\beta_2$ AR in cardiac myocytes (5). Specifically, PDE4D splicing variants have been implicated in association with  $\beta$ AR subtypes for receptor signaling and function (5).  $\beta_1$ AR forms a signaling complex with PDE4D8, which dissociates from the receptor upon agonist stimulation (6). Conversely, activation of  $\beta_2$ AR initiates recruitment of a complex consisting of  $\beta$ -arrestin and PDE4D5 (7, 8). However, the functional implication of this and other PDE4D isoforms in binding to  $\beta_2$ AR remains unclear. Here, we show that  $\beta_2$ AR binds to a set of PDE4D isoforms in distinct ways.  $\beta_2$ AR binds to both PDE4D9 and PDE4D8 at resting state, with PDE4D9 dissociation from the receptor and PDE4D8 recruitment to the receptor upon agonist stimulation. In addition, PDE4D5 is recruited to the activated  $\beta_2$ AR similar to that reported previously (7, 8). The differential association of PDE4D isoforms with  $\beta_2$ AR plays distinct roles in confining the receptor-induced cAMP activities for physiological contraction responses. Our data underscore the complexity of PDE regulation of cellular cAMP to enforce the specificity of  $\beta$ AR subtype signaling.

## MATERIALS AND METHODS

*Neonatal Cardiac Myocytes Isolation and Contraction Rate Assay*—Spontaneously beating neonatal cardiac myocytes were isolated from 1- to 2-day-old wild type or  $\beta_1$ AR-knock-out (KO) neonatal mice as described previously (9). Cells were cultured in Dulbecco's modified Eagle's medium (high glucose, 4.5 g/liter) supplemented with 10% fetal bovine serum, 1 mM glu-

\* This work was supported, in whole or in part, by National Institutes of Health Grant HL082846 (to Y. X.). This work was also supported by American Heart Association 0635331N (to Y. X.).

<sup>§</sup> The on-line version of this article (available at <http://www.jbc.org>) contains supplemental Figs. S1–S6.

<sup>1</sup> To whom correspondence should be addressed: Dept. of Molecular and Integrative Physiology, University of Illinois, 523 Burrill Hall, 407 S. Goodwin Ave., Urbana, IL 61801. Tel.: 217-265-9448; Fax: 217-333-1133; E-mail: kevinxy@illinois.edu.

<sup>2</sup> The abbreviations used are: PKA, protein kinase A; AR, adrenoceptor; FRET, fluorescence resonance energy transfer; PDE, phosphodiesterase; KO, knockout; DN, dominant negative; ANOVA, analysis of variance; GFP, green fluorescent protein; shRNA, short hairpin RNA.

tamine, 30  $\mu\text{g/ml}$  penicillin, and 100  $\mu\text{g/ml}$  streptomycin on plates precoated with 150 mg/ml gelatin type A and incubated at 37 °C with 5%  $\text{CO}_2$ . Measurement of spontaneous neonatal cardiac myocyte contraction rate was carried out as described previously (9).

**Adenovirus Preparation and Myocyte Infection**—The N-terminal sequences containing splicing regions from rat PDE4D1 to PDE4D9 were subcloned into pEGFP vector using the same strategy as described previously (3). The sequences from the N-end to the linker region (EQEDV<sup>254</sup> between UCR2 regions and catalytic domains in PDE4D3) were amplified by PCR and subcloned into pEGFP-N2 vector by HindIII/EcoRI sites. The aspartic acids in catalytic domains were replaced by alanine in PDE4D5, -4D8, and -4D9 isoforms to generate dominant negative PDE4Ds before fusing the mutant enzymes with mCherry at the C-terminal ends. Both GFP- and mCherry-fused PDE4D isoforms were cloned into the shuttle vector of the AdEasy<sup>TM</sup> system for virus production according to the manufacturer's instruction (MP Biomedical, Cleveland, OH). Recombinant adenovirus expressing FLAG-tagged  $\beta_2$ AR has been described previously (9). Neonatal myocytes, HEK293 fibroblasts, or mouse embryonic fibroblasts were infected with recombinant adenovirus expressing FLAG-tagged mouse  $\beta_2$ AR and/or individual PDE4D isoforms as indicated in the text. In controls, cells were infected with adenovirus encoding either GFP or mCherry.

**PDE4D shRNA Knockdown**—Forward and reverse oligonucleotides were synthesized (IDT DNA, Skokie, IL) for the following targets: PDE4D8 (forward, 5'-GATCCCCGGACC-ATCTCCAAGAACTATTCAAGAGATAGTTCTTGGAGATGGTCCCTTTTA-3'; reverse, 5'-AGCTTAAAAAGGACCA-TCTCCAAGAACTATCTCTTGAATAGTTCTTGGAGATGGTCCGGG-3'); PDE4D9 (forward, 5'-GATCCCCGCCAAGATCCAGGTCTACATTCAAGAGATGTAGACCTGGATCTTGGCTTTTTTA-3'; reverse, 5'-AGCTTAAAAAGCCAA-GATCCAGGTCTACATCTCTTGAATGTAGACCTGGATCTTGGCGGG-3'); and PDE4D9 control (forward, 5'-GAT-CCCCTGAGGACAACGGAGGCAGTTTCAAGAGAAC-TGCCTCCGTTGTCCTCATTTTTTA-3'; reverse, 5'-AGC-TTAAAAATGAGGACAACGGAGGCAGTTCTCTTGAA-ACTGCCTCCGTTGTCCTCAGGG-3'). Oligonucleotides were annealed at room temperature and ligated into pSuper vector with BglII and HindIII. The N-terminal sequences of mouse PDE4D8 or PDE4D9 were amplified from the cDNA library and fused with GFP on pEGFP-N1 vector. Myocytes were co-transfected with shRNAs and PDE4D8-GFP or PDE4D9-GFP at a DNA ratio of 10:1 (shRNA:PDE). After 24 h of expression, silencing efficiency was determined by fluorescence images of GFP expression and Western blot using GFP antibody. The PDE4D8, PDE4D9, or control shRNA was co-transfected with the ICUE3 probe into  $\beta_1$ AR-KO myocytes for FRET study.

**Drugs and Peptides**—Myocytes were treated with the  $\beta$ AR agonist isoproterenol (10  $\mu\text{M}$ , Sigma) as indicated. In some experiments, rolipram (10  $\mu\text{M}$ , Sigma) was used to pretreat myocytes for 10 min before isoproterenol stimulation. Membrane-permeable Tat peptide (GRKKRRQRRRPP) was linked to the 30 amino acids of N-terminal PDE4D8 or the 22 amino

acids of PDE4D9. Myocytes were pretreated with 10  $\mu\text{M}$  of peptides for 20 min before stimulation with isoproterenol.

**cAMP Measurement by FRET**—Myocytes were transfected with the indicator of cAMP using exchange protein activated by cAMP (ICUE) ICUE3 plasmid (10) together with PDE4D8 or PDE4D9 shRNA via Lipofectamine 2000 (Invitrogen) according to the manufacturer's protocol. The plasmid was designed by sandwiching a truncated cAMP-regulated guanine nucleotide exchange factor exchange protein activated by cAMP 2 with cyan fluorescent protein and a mutated yellow fluorescent protein cpVenus194. The truncated exchange protein activated by cAMP 2 lacks the N-terminal region containing amino acids 1–148. The resulting ICUE3 is a cytosolic protein with homogeneous expression in cardiac myocytes (data not shown). After 24 h expression, cells were rinsed and maintained in phosphate-buffered saline with calcium for FRET recording (11). Cells were imaged on a Zeiss Axiovert 200 M microscope with a 40 $\times$ /1.3NA oil-immersion objective lens and a cooled CCD camera. Dual emission ratio imaging was acquired with a 420DF20 excitation filter, a 450DRLP diachronic mirror, and two emission filters (475DF40 for cyan and 535DF25 for yellow). The acquisition was set with a 200-ms exposure in both channels and 20-s elapses. Images in both channels were subjected to background subtraction, and ratios of yellow-to-cyan color were calculated at different time points. The binding cAMP to ICUE3 led to decreases in the ratio yellow fluorescent protein/cyan fluorescent protein, which were plotted with inverted y axis.

**Co-immunoprecipitation and Western Blot**—After stimulation with isoproterenol, cells were rinsed with ice-cold phosphate-buffered saline and lysed in co-immunoprecipitation buffer (20 mM Hepes, pH 7.5, 150 mM NaCl, 2 mM EDTA, 10% glycerol, 0.6% Nonidet P-40, Thermo Halt protease, and phosphatase inhibitor mixture (Thermo Fisher Scientific, Inc.)). Lysates were rotated at 4 °C for 30 min, followed by centrifugation at 16,000  $\times g$  for 30 min. FLAG- $\beta_2$ ARs were immunoprecipitated using anti-FLAG M2 affinity resin (Sigma). The total immunoprecipitated proteins were resolved by SDS-PAGE and blotted with the following antibodies: anti-FLAG M1 (Sigma); anti- $\beta_2$ AR (SCBT); anti-phosphoserine 345 and 346 of  $\beta_2$ AR (SCBT); anti-GFP (Clontech); anti-RFP/mCherry (Rockland, PA), anti-PDE4-pan (Abcam); and anti- $\gamma$ -tubulin (Sigma). 5% of the lysate was loaded in the Western blots for immunoprecipitation experiments.

**Statistical Analysis**—Two-way ANOVA and Student's *t* test were performed using Prism (GraphPad software).

## RESULTS

**Association of PDE4D9 and PDE4D8 with  $\beta_2$ AR in Cardiac Myocytes at Resting State**—Our previous study has identified that phosphodiesterase 4D gene functionally associates with  $\beta_2$ ARs in cardiac myocytes (5). Among nine PDE4D splicing isoforms, seven are expressed in animal heart (3). Using the FLAG- $\beta_2$ AR, we pulled down the endogenous PDE4D isoforms with the strongest staining corresponding to PDE4D3, -4D8, and -4D9 on Western blots (Fig. 1A). The N-terminal regions of PDE4D isoforms contain the specific sequences important for subcellular distribution and/or protein interaction (2). To iden-

## Phosphodiesterase Regulates $\beta_2$ -Adrenoceptor Signaling

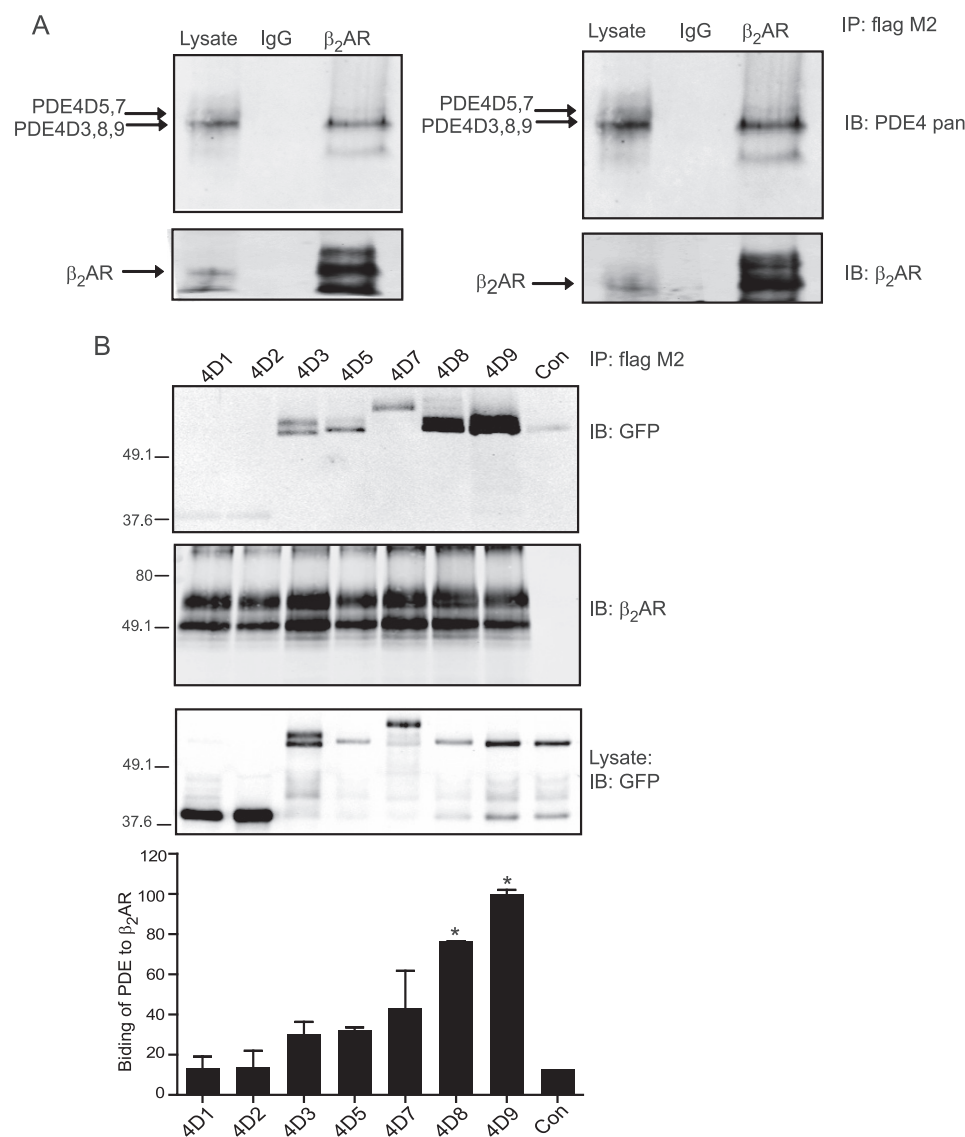


**FIGURE 1. PDE4D9 and PDE4D8 preferentially bind to  $\beta_2$ AR in cardiac myocytes.** *A*, FLAG- $\beta_2$ AR is expressed in wild type neonatal myocytes. The immunoprecipitated (IP)  $\beta_2$ AR and the bound endogenous PDE4D proteins are examined by Western blotting with indicated antibodies. *IB*, immunoblot. *B*, FLAG- $\beta_2$ AR and GFP-PDE4Ds (the N-terminal fragments from rat 4D1 to 4D9) are co-expressed in  $\beta_1$ AR-KO myocytes. The immunoprecipitated  $\beta_2$ AR and the bound GFP-PDE4D proteins are examined by Western blotting with the indicated antibodies. The Western blots are quantified and normalized against the control (Con) without  $\beta_2$ AR expression ( $n = 3$ ); \*,  $p < 0.05$  when compared with the control by Student's *t* test. In each gel, the total immunoprecipitates are loaded, and the lysate loading represents 5% of the total.

tify the specific PDE4D isoforms that associate with  $\beta_2$ AR in cardiac myocytes, we expressed the N-terminal fragments of the seven cardiac PDE4D isoforms together with FLAG- $\beta_2$ AR in wild type myocytes. Both PDE4D8 and PDE4D9 were preferentially pulled down together with  $\beta_2$ AR, with PDE4D9 displaying more binding than PDE4D8 (Fig. 1*B*). In comparison, PDE4D3, -4D5, and -4D7 displayed a small amount of association with  $\beta_2$ AR, whereas PDE4D1 and -4D2 did not bind to the receptor. The interaction appears to be myocyte-specific because a similar experiment in HEK293 fibroblasts showed that FLAG- $\beta_2$ AR bound most of the PDE4D isoforms without discrimination (supplemental Fig. S1). Together, these data identified that PDE4D9, and to a lesser extent PDE4D8, forms complexes with the  $\beta_2$ AR at resting condition in cardiac myocytes.

*Association of PDE4D9 and PDE4D8 with  $\beta_2$ AR Regulates Receptor Signaling-induced Contraction Rate Response in Cardiac Myocytes*—When the N-terminal fragments of PDE4D isoforms were overexpressed, they should function in a dominant negative fashion by competing against the endogenous enzymes for subcellular distribution. We examined the functional implication by overexpressing the N terminus of PDE4D isoforms lacking the catalytic domain in  $\beta_1$ AR-KO myocytes. The N terminus of PDE4D isoforms displayed similar cellular distribution between wild type and  $\beta_1$ AR-KO cardiac myocytes (supplemental Fig. S2), indicating that the lack of endogenous  $\beta_1$ AR does not affect the distribution of PDE4D isoforms. Consistent with co-immunoprecipitation data, the overexpressed N terminus of PDE4D9 displayed more overlap with FLAG- $\beta_2$ AR than those of PDE4D8 and PDE4D5, indicating a relatively preserved integrity of signaling complex composition in cardiac myocytes (supplemental Fig. S3).

Overexpression of the N terminus of PDE4D9 (PDE4D9-GFP) or PDE4D8 (PDE4D8-GFP) significantly enhanced contraction rate increases induced by 10  $\mu$ M isoproterenol in  $\beta_1$ AR-KO myocytes (maximal increase of  $14.1 \pm 2.2$ ,  $23.3 \pm 3.5$ , and  $22.5 \pm 2.7$  beats/min for control, PDE4D8, and PDE4D9, respectively; see Fig. 2, *A* and *B*). Overexpressing PDE4D5-GFP had no effect on the maximal contraction rate increase, although it had a small enhancing effect on the response after extended stimulation (Fig. 2*C*). In contrast, overexpressing GFP alone or any other PDE4D isoforms had minimal effect on enhancing myocyte contraction rate responses induced by isoproterenol. PDE4D2 actually attenuated the contraction rate response (Fig. 2, *D–H*). Together, these data identified PDE4D9 and PDE4D8 as the critical isoforms for the receptor signaling-induced myocyte contraction rate responses.

To verify the functional roles of PDE4D9 and PDE4D8 in  $\beta_2$ AR signaling, we delivered membrane-permeable Tat-conjugated peptide containing either the N-terminal 30 PDE4D8-specific amino acids (pep-4D8) or 22 PDE4D9-specific amino acids (pep-4D9) into cardiac myocytes to perturb the subcellular distribution of the corresponding PDE4D isoforms. Accordingly, delivering the

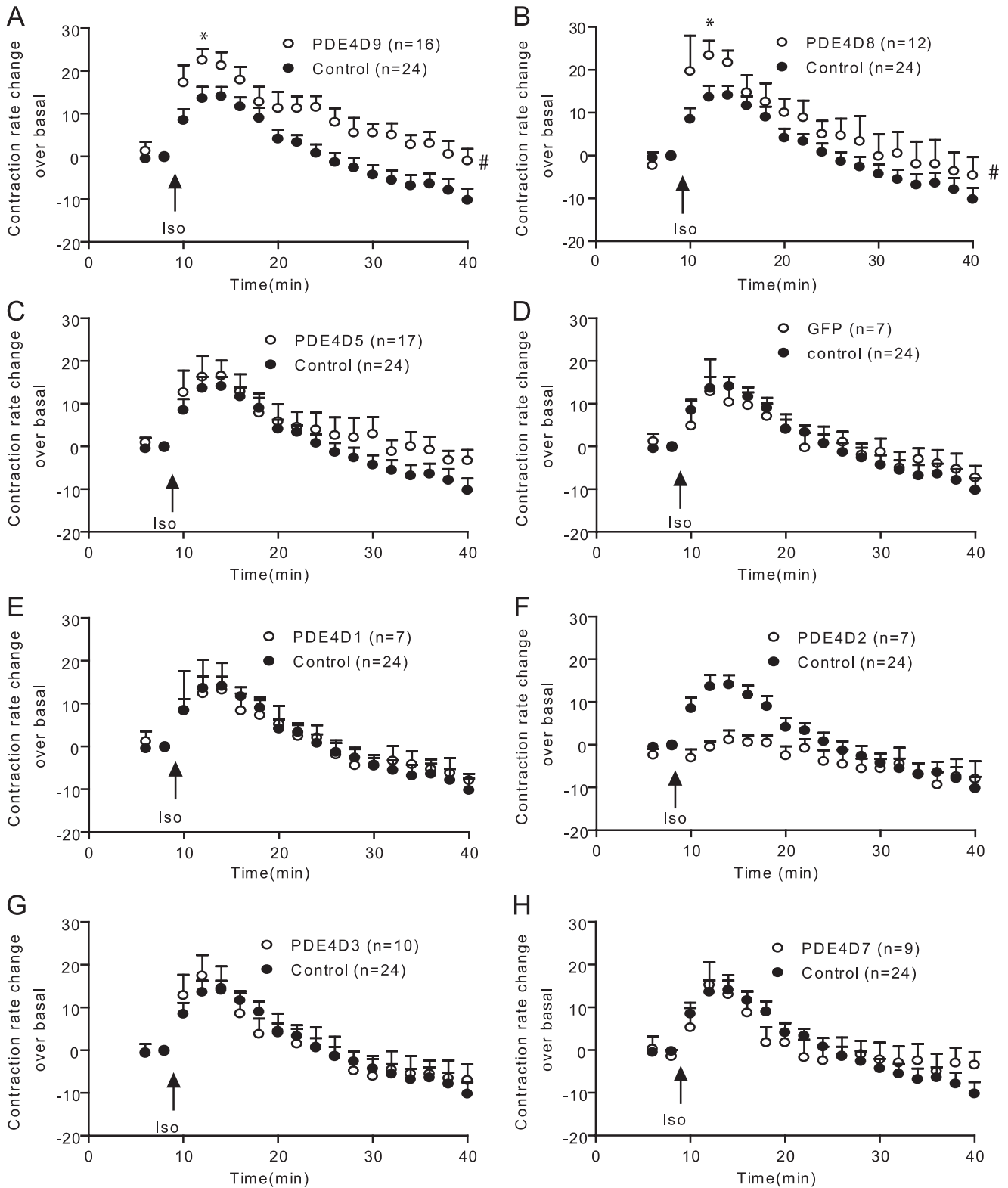
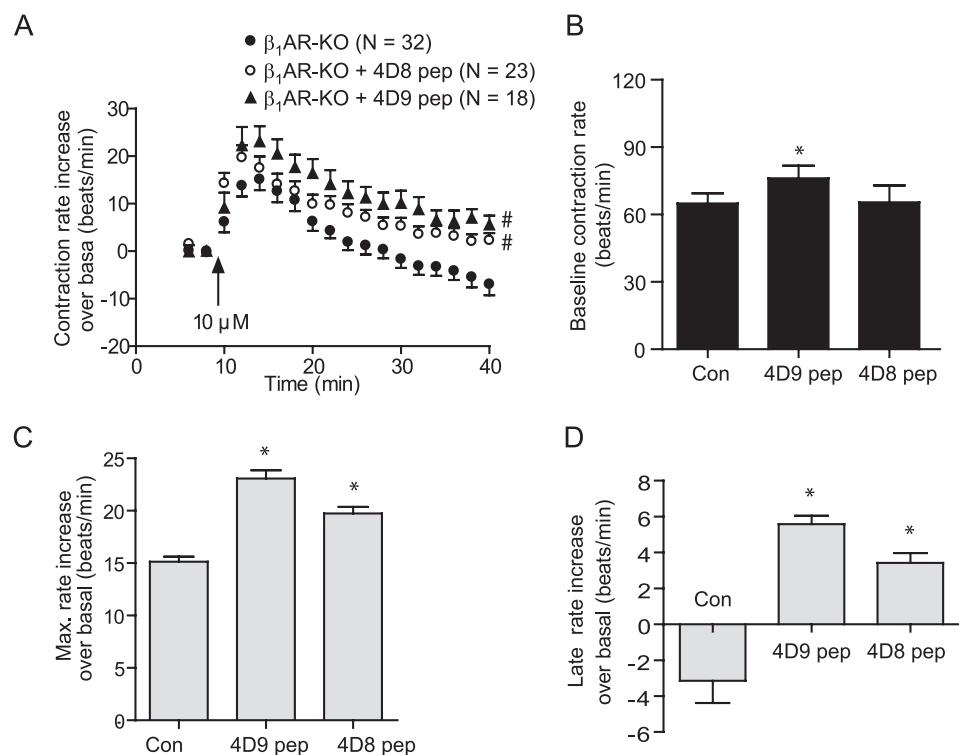


FIGURE 2. PDE4D9 and PDE4D8 regulate the  $\beta_2$ AR-induced contraction rate responses in  $\beta_2$ AR-KO neonatal myocytes. Myocytes expressing the rat N-terminal GFP-PDE4D9 (A) and GFP-PDE4D8 (B), GFP-PDE4D5 (C), the GFP control (D), or other GFP-PDE4Ds (4D1, 4D2, 4D3, and 4D7, E-H, respectively) are stimulated with 10  $\mu$ M isoproterenol (Iso). The myocyte contraction rates are measured, and the time courses of changes in contraction rates are plotted. #,  $p < 0.05$  when compared with the control by two-way ANOVA. \*,  $p < 0.05$  when compared with the control by Student's *t* test.

membrane-permeable peptide pep-4D9 and pep-4D8 significantly enhanced the contraction rate increases induced by 10  $\mu$ M isoproterenol (maximal increase of  $15.2 \pm 2.2$ ,  $19.7 \pm 2.6$ , and

$23.1 \pm 3.2$  beats/min for the control, pep-4D8, and pep-4D9, respectively; see Fig. 3). Delivery of either peptide had minimal effects on base-line levels of contraction rate (Fig. 3B).

## Phosphodiesterase Regulates $\beta_2$ -Adrenoceptor Signaling



**FIGURE 3. Perturbation of PDE4D9 and PDE4D8 with membrane-permeable peptide alters the  $\beta_2$ AR-induced myocyte contraction rate increases.**  $\beta_1$ AR-KO myocytes treated with membrane-permeable peptide pep-4D9 and pep-4D8 are stimulated with  $10 \mu\text{M}$  isoproterenol (*Iso*). *A*, myocyte contraction rates are measured, and the time courses of changes in contraction rates are plotted. The base-line contraction rate (*B*) and the maximal increases in contraction rate (*C*) in *A* are plotted. *D*, contraction rate increases after 30 min of extended stimulation in *A* are plotted. #,  $p < 0.05$  when compared with the control (*Con*) by two-way ANOVA. \*,  $p < 0.05$  when compared with the control by Student's *t* test.

**PDE4D9 and PDE4D8 Differentially Control cAMP Levels Induced by  $\beta_2$ AR Activation in Cardiac Myocytes**—Previous studies have indicated that the cAMP signal induced by  $\beta_2$ AR activation is restricted in local environments and is subjected to rapid degradation by the surrounding PDE activities (12, 13). Our functional data suggest that PDE4D8 and -4D9 isoforms are responsible for degradation of the  $\beta_2$ AR-induced cAMP. Thus, we applied the FRET-based cAMP indicator ICUE3 to measure cAMP accumulation induced by the endogenous  $\beta_2$ AR in  $\beta_1$ AR-KO cardiac myocytes.

Meanwhile, we developed PDE4D8- and -4D9-specific shRNA to knock down the respective isoforms in neonatal cardiac myocytes (Fig. 4, *A* and *B*). Stimulation of the endogenous  $\beta_2$ AR with isoproterenol induced a robust and transient increase of cAMP FRET response in  $\beta_1$ AR-KO myocytes (maximal increase of  $0.26 \pm 0.03$ ; see Fig. 4*C*). However, co-expressing PDE4D9-specific shRNA significantly enhanced the maximal cAMP FRET increase (maximal increase of  $0.37 \pm 0.06$ ; see Fig. 4*C*), whereas co-expressing PDE4D8-specific shRNA did not affect the maximal cAMP FRET increase (maximal increase of  $0.27 \pm 0.06$ ), but it slowed the decrease after reaching peak levels ( $t_{1/2}$  of  $86.1 \pm 1.2$  and  $167 \pm 3.9$  s for the control and PDE4D8 shRNA, respectively; see Fig. 4*D*). In contrast, overexpression of control shRNA did not affect the cAMP FRET responses (maximal increase of  $0.25 \pm 0.05$ ; see Fig. 4*E*), whereas inhibition of all PDE4 activities with rolipram significantly enhanced the maximal cAMP FRET increase, and pro-

longed the increase during extended stimulation (Fig. 4*F* and data not shown). Together, these data indicate differential contribution of individual PDE4 enzymes in controlling intracellular cAMP signaling. Although the  $\beta_2$ AR-associated PDE4D9 controls the maximal cAMP increase under  $\beta_2$ AR stimulation, other PDE4s can modulate the duration of the cAMP responses induced by  $\beta_2$ AR.

**Agonist-dependent Association between PDE4D Isoforms and  $\beta_2$ AR in Cardiac Myocytes**—To further understand the effects on interaction between PDE4D isoforms and  $\beta_2$ AR, we examined a time course of association between PDE4D isoforms and  $\beta_2$ AR after stimulation with isoproterenol. Similar to those observed in the Fig. 1, PDE4D9 displayed significant binding to the  $\beta_2$ AR at resting condition. However, the association was significantly decreased upon stimulation of the receptor with isoproterenol (Fig. 5). In contrast, both PDE4D5 and PDE4D8 had a lower amount of binding to the  $\beta_2$ AR at resting state, but the association was significantly

increased upon stimulation with isoproterenol. Consistent with the previous report (7, 8), the recruitment of PDE4D5 to the activated  $\beta_2$ AR peaked at 5 min of stimulation (Fig. 5). The recruitment of PDE4D8 to the receptor peaked at 10 min after stimulation (Fig. 5), which appears to be opposing the dissociation of PDE4D8 from the activated  $\beta_1$ ARs previously reported in HEK293 cells (6). Indeed, full-length PDE4D8 displayed an agonist-dependent dissociation from the activated  $\beta_1$ ARs in myocytes, whereas PDE4D9 did not bind to  $\beta_1$ ARs at all (supplemental Fig. S4). The recruitment of both PDE4D5 and -4D8 to the activated  $\beta_2$ AR were dependent on  $\beta$ -arrestin (supplemental Fig. S5). In mouse embryonic fibroblast cells lacking both  $\beta$ -arrestin 1 and -2, neither PDE4D5 nor 4D8 bound to the activated  $\beta_2$ ARs (supplemental Fig. S5). Reintroducing expression of  $\beta$ -arrestin 2 rescued the agonist-dependent binding of PDE4D8 to the  $\beta_2$ ARs (supplemental Fig. S5). In contrast, the binding of full-length PDE4D9 to the  $\beta_2$ ARs was not enhanced by receptor activation in wild type mouse embryonic fibroblast cells; interestingly, the binding was also reduced by gene deficiency of  $\beta$ -arrestin 1 and -2 (supplemental Fig. S6).

The cAMP signals under the control of PDE4D isoforms could affect the PKA activities for protein phosphorylation within the  $\beta_2$ AR complexes. We then examined the receptor phosphorylation by PKA in cardiac myocytes. A single amino acid mutation was introduced into catalytic domains to abolish enzymatic activity of PDE4D, which functions as a dominant negative (PDE4-DN) (7). Overexpressing PDE4D9-DN, but not

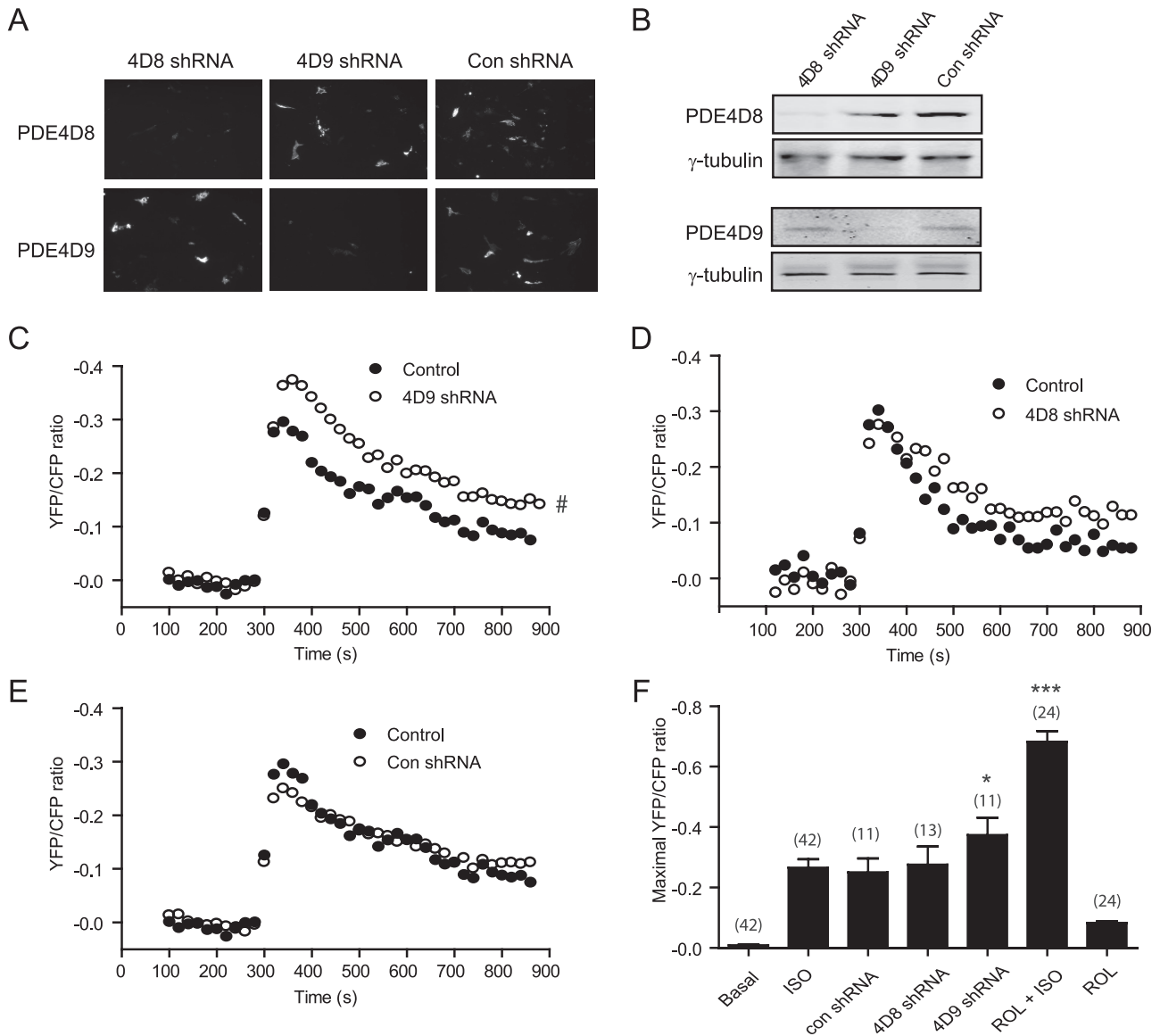


**FIGURE 4. Knockdown of PDE4D9 and PDE4D8 affects the  $\beta_2$ AR-induced cAMP accumulation in cardiac myocytes.**  $\beta_1$ AR-KO myocytes overexpressing mouse GFP-PDE4D isoforms together with the control (Con) or specific shRNAs for PDE4D9 or PDE4D8 are harvested. The protein levels of GFP-PDE4D are examined by imaging (A) and Western blot (B). In  $\beta_1$ AR-KO myocytes, ICUE3 is co-transfected with either PDE4D9 shRNA (C), PDE4D8 shRNA (D), or the control shRNA (E); and cells are stimulated with 10  $\mu$ M isoproterenol. The time courses of changes in ICUE3 FRET ratio are measured and plotted. F, maximal increases in the FRET ratio induced by stimulation with 10  $\mu$ M isoproterenol from C–E or after inhibition of PDE4 activities are plotted. #,  $p < 0.05$  when compared with the control by two-way ANOVA. \*,  $p < 0.05$  and \*\*\*,  $p < 0.001$  when compared with the control by Student's *t* test. ISO, isoproterenol; ROL, rolipram.

PDE4D5-DN and PDE4D8-DN, significantly enhanced the PKA phosphorylation at serine 345/346 of the  $\beta_2$ AR expressed in  $\beta_1$ AR-KO myocytes (Fig. 6A). After stimulation with isoproterenol, overexpression of PDE4D9-DN significantly enhanced the PKA phosphorylation of the  $\beta_2$ ARs at serine 345/346, whereas PDE4D8-DN had a small enhancement on the PKA phosphorylation (Fig. 6B). Moreover, overexpressing PDE4D9-DN and PDE4D5-DN but not PDE4D8-DN significantly enhanced base-line levels of contraction rates (Fig. 7, A–C and E). Upon agonist stimulation, overexpressing PDE4D9-DN and PDE4D8-DN but not PDE4D5-DN significantly enhanced the maximal contraction rate increases induced by  $\beta_2$ AR activation (Fig. 7, A, B, and D). In contrast, overexpressing wild type PDE4D5, -4D8, and -4D9 had minimal effect on both base-line and maximal contraction rate increases induced by isoprotere-

nol in  $\beta_1$ AR-KO myocytes (Fig. 7, C and D). Together, these data suggest that PDE4D isoforms have differential association with  $\beta_2$ ARs and control the receptor-associated cAMP activities for contraction rate changes at both resting state and under stimulation.

## DISCUSSION

PDE4D isoforms play an essential role in regulating local cAMP/PKA activities induced by a variety of neurotransmitters and hormones. In this study, we have characterized novel signaling complexes associated with  $\beta_2$ AR in cardiac myocytes. In contrast to the preferential association of PDE4D8 with the  $\beta_1$ AR in HEK293 fibroblasts (6),  $\beta_2$ AR displays diversified association with multiple PDE4D isoforms in cardiac myocytes (Fig. 8). At resting state,  $\beta_2$ AR preferentially associates with PDE4D9

## Phosphodiesterase Regulates $\beta_2$ -Adrenoceptor Signaling

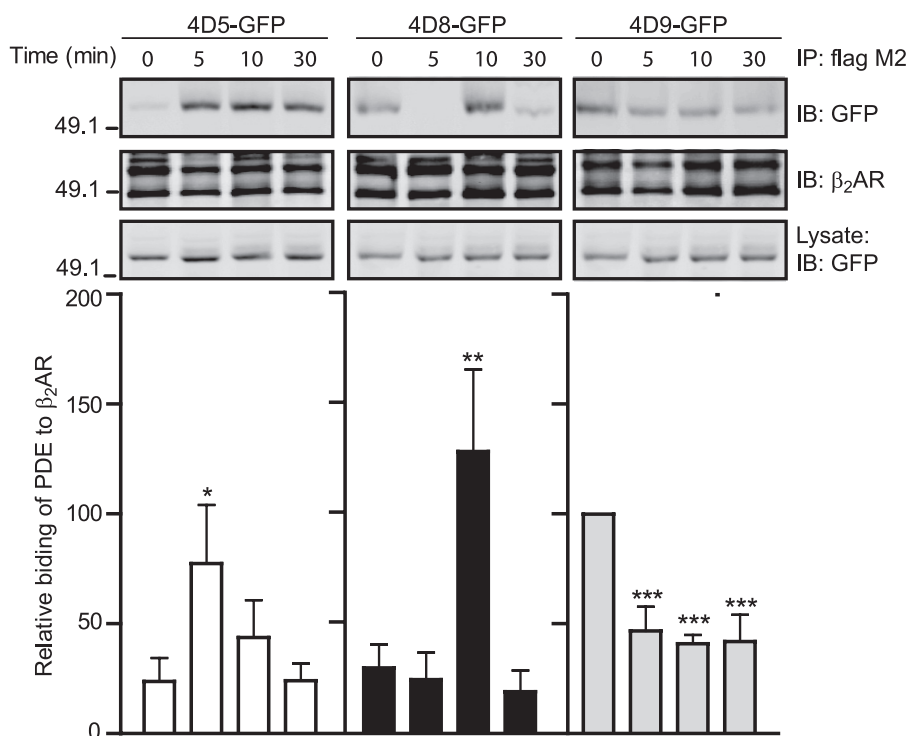


**FIGURE 5. Activation of  $\beta_2$ AR induces dynamic interaction between the receptor and PDE4D isoforms in myocytes.**  $\beta_2$ AR-KO expressing FLAG- $\beta_2$ AR and PDE4D-GFP fusion proteins (4D5, 4D8, and 4D9) are treated with 10  $\mu$ M isoproterenol (*Iso*) at the indicated time. The immunoprecipitated (*IP*) FLAG- $\beta_2$ AR and the bound PDE4D proteins are blotted with the indicated antibodies. The Western blots are quantified and plotted against the base-line levels of individual isoforms ( $n = 3$ ). \*,  $p < 0.05$ ; \*\*,  $p < 0.005$ ; and \*\*\*,  $p < 0.001$  when compared with the respective base-line control by Student's *t* test. In each gel, the total immunoprecipitates are loaded, and the lysate loading represents 5% of the total. *IB*, immunoblot.

and to a less extent PDE4D8. However, PDE4D9 is dissociated from the receptor upon stimulation, whereas both PDE4D8 and PDE4D5 are recruited to the receptor in a  $\beta$ -arrestin-dependent manner, likely through binding to  $\beta_2$ AR/ $\beta$ -arrestin complexes (supplemental Fig. S5) (8). These divergent complex formations concur with the preferential activation of PDE4D5, -4D8, and -4D9 upon  $\beta_2$ AR signaling in cardiac myocytes (6). Thus, under basal conditions, PDE4D9 and to a lesser degree PDE4D8 are poised to control local cAMP concentration and PKA activity in the vicinity of  $\beta_2$ AR (Fig. 6), whereas PDE4D5 and PDE4D8 likely affect  $\beta_2$ AR signaling after ligand binding and  $\beta$ -arrestin recruitment. The fate and function of the released PDE4D9 are to be determined and may provide a means to regulate a distinct pool of cAMP away from the membrane. The striking and diversified association between PDE4D isoforms and  $\beta_2$ AR likely impacts the time course of cAMP signals in the vicinity of the receptors, which supports the divergent signaling pathways emanating from the  $\beta_2$ AR (1). Together with a previous report on PDE4D8 binding to  $\beta_1$ AR (6), our data indicate that  $\beta_1$ - and  $\beta_2$ AR differ in terms of the PDE4D splicing variant recruitment to the receptor, the mode of interaction with the PDE4D variants, and the effect of receptor agonist on the complexes.

Under basal conditions, binding of PDE4D to  $\beta_2$ ARs can facilitate cAMP hydrolysis in the vicinity of the unoccupied receptors and prevent a local increase of cAMP, which may have different functional implications. First, it can protect  $\beta_2$ ARs from PKA-mediated phosphorylation (14). Second, it may control PKA-mediated phosphorylation of other substrates such as the L-type calcium channel (15) in the receptor complexes and/or local signaling microdomains, thus keeping the system at resting condition. Third, it may maintain receptor/G protein coupling fidelity by preventing PKA phosphorylation-

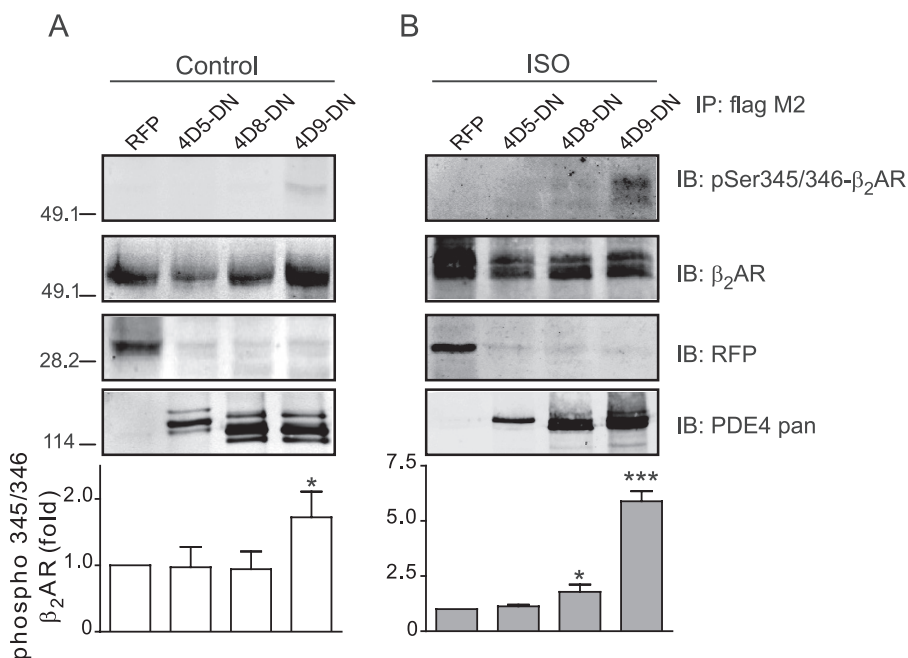


**FIGURE 6. Dominant negative PDE4D9 and PDE4D8 enhance the PKA phosphorylation of the  $\beta_2$ AR.** Dominant negative (*DN*) PDE4D isoforms are expressed together with FLAG- $\beta_2$ AR in  $\beta_1$ AR-KO myocytes. Cells are treated with 10  $\mu$ M isoproterenol. The FLAG- $\beta_2$ AR is immunoprecipitated (*IP*) and detected with antibody against PKA phosphorylation sites (Ser-345 and Ser-346) or as indicated. The data are quantified and plotted against the red fluorescence protein control ( $n = 3$ ). \*,  $p < 0.05$  and \*\*\*,  $p < 0.001$  when compared with the RFP control by Student's *t* test. In each gel, the total immunoprecipitates are loaded, and the lysate loading represents 5% of the total. *IB*, immunoblot.

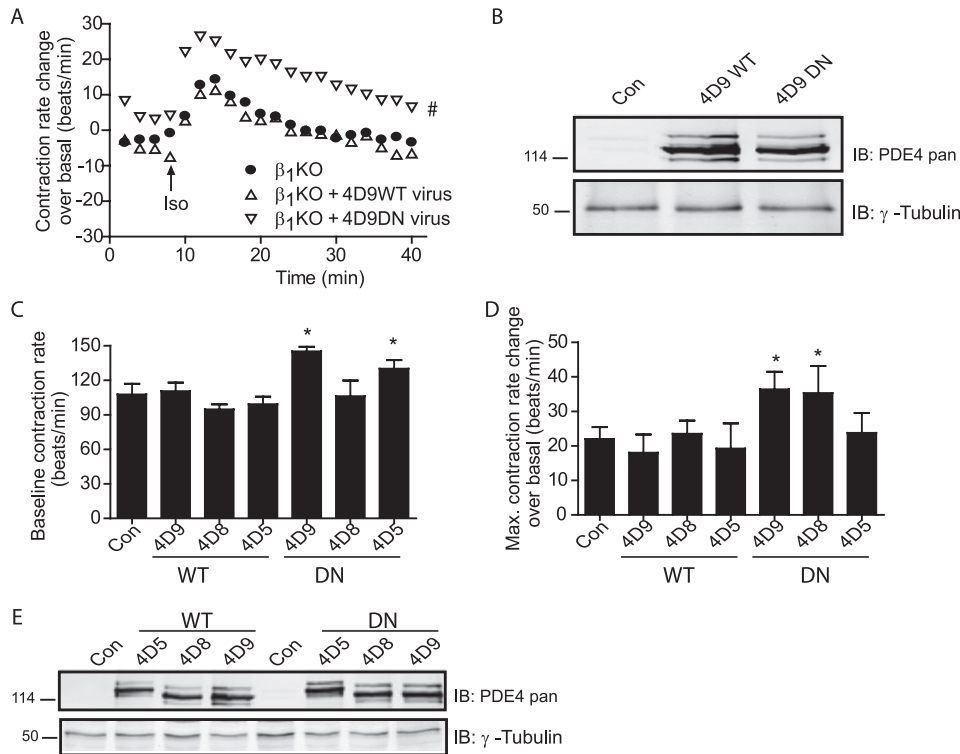


**FIGURE 7. Dominant negative PDE4D isoforms affect the  $\beta_2$ AR signaling for myocyte contraction rate.** *A*,  $\beta_1$ AR-KO myocytes expressing DN-PDE4D9 (4D9DN) or wild type PDE4D9 (4D9WT) are stimulated with isoproterenol (10  $\mu$ M). The time courses of changes in myocyte contraction rates are plotted. *B*, expression of both PDE4D9-WT and PDE4D9-DN in *A* are examined in Western blotting with the indicated antibodies. *C–E*,  $\beta_1$ AR-KO myocytes expressing DN-PDE4D isoforms or their corresponding wild type PDE4D isoforms are stimulated with isoproterenol (10  $\mu$ M). The changes in myocyte contraction rates are measured. The changes in the base line (*C*) and the changes in the maximal contraction rate (*D*) are plotted against the mCherry control (Con). *E*, expression of WT and DN-PDE4D isoforms in *C* and *D* are examined in Western blotting with indicated antibodies. #,  $p < 0.05$  when compared with the control by two-way ANOVA. \*,  $p < 0.05$  when compared with the control by Student's *t* test. IB, immunoblot.

dependent switching of receptor coupling from  $G_s$  to  $G_i$  (16). Indeed, when PDE4D9 activity is knocked down with shRNA (Fig. 4C), we observe a substantial increase in the  $\beta_2$ AR-induced cAMP, although the increase is still below that from inhibition of total PDE4 activities with rolipram (Fig. 4F). In contrast, inhibition of PDE4D8 activity with shRNA knockdown leads to minimal alteration of the maximal cAMP signal induced by  $\beta_2$ AR but with slower attenuation (Fig. 4D). Consistent with this view, localized cAMP transients are elevated in the PDE4D knock-out myocytes, whereas global cAMP signaling is not perturbed (17).

Consequently,  $\beta_2$ AR phosphorylation is differentially regulated by PDE4D isoforms at basal and stimulatory conditions. Inhibition of PDE4D9 leads to increases in PKA phosphorylation of the receptor at both basal and stimulatory conditions, whereas inhibition of PDE4D8 only has a small enhancement effect after agonist stimulation (Fig. 6). Interestingly, stimulation of  $\beta_1$ AR, the primary  $\beta$ AR subtype for cardiac contraction, causes dissociation of PDE4D8 from the receptor complex (supplemental Fig. S4) (6). It is thus plausible that simultaneous stimulation of both  $\beta_1$ - and  $\beta_2$ ARs can lead to switching PDE4D8 from  $\beta_1$ AR to  $\beta_2$ AR via arrestin-dependent mechanisms, which cooperates to produce a localized increase in cAMP in the proximity of the activated  $\beta_1$ ARs. This event should decrease local cAMP degradation

and therefore promote the  $\beta_1$ -adrenergic signal for contraction responses. Consistent with this notion, co-activation of  $\beta_1$ - and  $\beta_2$ ARs leads to synergistic stimulation of  $\beta_1$ AR-induced myocyte contractile response (18).

Using myocyte contraction rate changes in response to  $\beta$ -adrenergic stimulation as readout, we show that selective disruption of PDE4D isoform association with  $\beta_2$ ARs differentially affects the receptor signaling for physiological responses. Perturbation of PDE4D5 and PDE4D9 activity by overexpressing PDE4D-DN (Fig. 7) induces a substantial increase in basal contraction rate. The PDE4D9 effect is most likely due to altered cAMP levels and PKA phosphorylation within  $\beta_2$ AR complexes. The PDE4D5 effect may in part reflect the non-specific increase in cytosolic cAMP and PKA phosphorylation of proteins away from the receptor complexes, because displacing PDE4D5 activity with dominant negative PDE4D5 does not affect PKA phosphorylation of  $\beta_2$ AR (Fig. 6). When PDE4D9 activity is displaced by either overexpressing PDE4D9-DN or by membrane-permeable pep-

ptide, we observe a substantial increase in the maximal contraction rates under  $\beta_2$ AR stimulation (Figs. 3 and 7). The perturbation of PDE4D8 activity with dominant negative or membrane-permeable peptide induces a smaller but significant enhancement on the maximal contraction rate increases (Figs. 3 and 7). These data support the essential roles of PDE4D9 and to a lesser degree the PDE4D8 isoform in controlling the  $\beta_2$ AR-stimulated cAMP/PKA activity for cardiac contraction. The effects of membrane-permeable peptide also support the critical roles of the splicing sequences of PDE4D9 and PDE4D8 for receptor signaling. Our data may also underscore potential differences in the effects of acute treatment with the peptides versus overexpression of dominant negatives on PDE4D isoforms. With dominant negative proteins, additional sequences from individual PDE4D isoforms containing both UCR1 and UCR2 regulatory regions as well as the inactive catalytic domains may play a role on the observed effects.

In addition, perturbation of PDE4D2 attenuates the  $\beta_2$ AR-induced myocyte contraction rate response. PDE4D2 is a supershort isoform that lacks most of the regulatory domains and localization signature (3), and it may be constitutively active in the cytosol to interfere with diffusion of cAMP/PKA activity to downstream signaling proteins for contraction responses. Although PDE4D5 does not appear to play a role in regulating  $\beta_2$ AR-stimulated contraction response, this specific



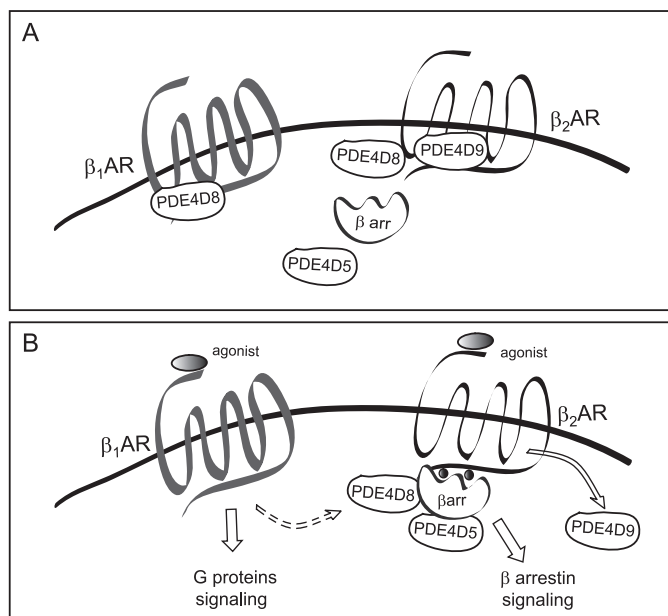


**FIGURE 8. Schematic models of differential association of PDE4D isoforms with  $\beta$ AR subtypes in cardiac myocytes.** *A*, at resting state, both  $\beta_1$ AR and  $\beta_2$ AR form signaling complexes with distinct PDE4D isoforms; PDE4D8 associates with  $\beta_1$ AR (6), whereas PDE4D9 and to a lesser extent PDE4D8 associate with  $\beta_2$ AR (Fig. 1). The binding of PDE4D isoforms to the receptors control local cAMP/PKA activities in the receptor microdomains. *B*, upon ligand stimulation, PDE4D8 is dissociated from the  $\beta_1$ AR, whereas PDE4D9 is dissociated from the  $\beta_2$ AR. Interestingly, PDE4D8 and another splicing variant, PDE4D5, are recruited to the  $\beta_2$ AR via arrestin-dependent mechanism after receptor occupancy. It is thus plausible that simultaneous stimulation of both  $\beta_1$ - and  $\beta_2$ ARs can lead to switching PDE4D8 from  $\beta_1$ AR to  $\beta_2$ AR via arrestin-dependent mechanism, which cooperates to produce a localized increase in cAMP in the proximity of the activated  $\beta_1$ ARs. This event should synergistically promote the  $\beta_1$ AR signal for myocyte contraction responses.

isoform may control the activity of the exchange protein activated by cAMP and/or extracellular signal-regulated kinase (ERK) (7, 8). In addition, the recruitment of PDE4D5 and PDE4D8 to the activated receptors can result in a local increase in PDE4 activity and therefore lower cAMP/PKA activities on receptor-containing endosomes to facilitate the receptor dephosphorylation for subsequent recycling.

Together, our findings demonstrate that PDE4D9 and PDE4D8 are preferentially associated with  $\beta_2$ AR at resting state in cardiac myocytes. Stimulation of  $\beta_2$ AR has divergent effects on PDE4D recruitment in the membrane subdomains, with PDE4D9 dissociating from the receptor and PDE4D8 and

PDE4D5 recruiting to the activated receptor. The dynamic localization of different PDE4D splicing variants, as well as their activation state, likely plays a major role in controlling cAMP accumulation in distinct subcellular domains.

*Acknowledgments*—We thank members of Xiang laboratory for comments and critically reading the manuscript and Dr. Jin Zhang of The Johns Hopkins University for the ICUE3 constructs.

**REFERENCES**

- Xiao, R. P., Zhu, W., Zheng, M., Cao, C., Zhang, Y., Lakatta, E. G., and Han, Q. (2006) *Trends Pharmacol. Sci.* **27**, 330–337
- Conti, M., and Beavo, J. (2007) *Annu. Rev. Biochem.* **76**, 481–511
- Richter, W., Jin, S. L., and Conti, M. (2005) *Biochem. J.* **388**, 803–811
- Zaccolo, M., and Pozzan, T. (2002) *Science* **295**, 1711–1715
- Xiang, Y., Naro, F., Zoudilova, M., Jin, S. L., Conti, M., and Kobilka, B. (2005) *Proc. Natl. Acad. Sci. U.S.A.* **102**, 909–914
- Richter, W., Day, P., Agrawal, R., Bruss, M. D., Granier, S., Wang, Y. L., Rasmussen, S. G., Horner, K., Wang, P., Lei, T., Patterson, A. J., Kobilka, B., and Conti, M. (2008) *EMBO J.* **27**, 384–393
- Perry, S. J., Baillie, G. S., Kohout, T. A., McPhee, I., Magiera, M. M., Ang, K. L., Miller, W. E., McLean, A. J., Conti, M., Houslay, M. D., and Lefkowitz, R. J. (2002) *Science* **298**, 834–836
- Baillie, G. S., Sood, A., McPhee, I., Gall, I., Perry, S. J., Lefkowitz, R. J., and Houslay, M. D. (2003) *Proc. Natl. Acad. Sci. U.S.A.* **100**, 940–945
- Wang, Y., De Arcangelis, V., Gao, X., Ramani, B., Jung, Y. S., and Xiang, Y. (2008) *J. Biol. Chem.* **283**, 1799–1807
- Allen, M. D., DiPilato, L. M., Rahdar, M., Ren, Y. R., Chong, C., Liu, J. O., and Zhang, J. (2006) *ACS Chem. Biol.* **1**, 371–376
- Soto, D., De Arcangelis, V., Zhang, J., and Xiang, Y. (2009) *Circ. Res.* **104**, 770–779
- Xiang, Y., Rybin, V. O., Steinberg, S. F., and Kobilka, B. (2002) *J. Biol. Chem.* **277**, 34280–34286
- Zhou, Y. Y., Cheng, H., Bogdanov, K. Y., Hohl, C., Altschuld, R., Lakatta, E. G., and Xiao, R. P. (1997) *Am. J. Physiol.* **273**, H1611–H1618
- Tran, T. M., Friedman, J., Qunaibi, E., Baameur, F., Moore, R. H., and Clark, R. B. (2004) *Mol. Pharmacol.* **65**, 196–206
- Davare, M. A., Avdonin, V., Hall, D. D., Peden, E. M., Burette, A., Weinberg, R. J., Horne, M. C., Hoshi, T., and Hell, J. W. (2001) *Science* **293**, 98–101
- Daaka, Y., Luttrell, L. M., and Lefkowitz, R. J. (1997) *Nature* **390**, 88–91
- Lehnart, S. E., Wehrens, X. H., Reiken, S., Warriar, S., Belevych, A. E., Harvey, R. D., Richter, W., Jin, S. L., Conti, M., and Marks, A. R. (2005) *Cell* **123**, 25–35
- Zhu, W. Z., Chakir, K., Zhang, S., Yang, D., Lavoie, C., Bouvier, M., Hébert, T. E., Lakatta, E. G., Cheng, H., and Xiao, R. P. (2005) *Circ. Res.* **97**, 244–251